

CRACK PROPAGATION STUDIES IN AUSTENITIC STAINLESS STEEL IN HOT CORROSIVE FLUE GASES CONTAINING VANADIUM

S. Ramakrishna Iyer, K. J. L. Iyer and V. M. Radhakrishnan

Metallurgy Department, Indian Institute of Technology, Madras, India

ABSTRACT

The effect of vanadium content in flue gases on cracking and crack propagation in 304 type stainless steel at 550°C has been studied. Kerosene was used as the base fuel and vanadium content was varied from zero to 40 ppm. It has been observed that increasing vanadium upto around 20 ppm reduced the crack initiation time, increased the propagation rate and decreased the threshold stress intensity factor. Beyond 20 ppm of vanadium the trend is slightly reversed, thereby showing that there is a critical value of vanadium content in the flue gases for the worst attack. Cracking has been found to be intergranular. A probable mechanism of cracking and crack propagation is discussed.

KEYWORDS

Crack propagation, hot corrosion, 304 type stainless steel, vanadium attack, threshold stress intensity factor.

INTRODUCTION

Most of the alloys which are used for high temperature application are susceptible to hot corrosion attack to some degree. At elevated temperatures the presence of even air will affect the strength of an alloy through oxidation. High temperature operation with combustion gases from petroleum fuels involves the presence of sulphur, vanadium and sodium derived from the crude or from catalysts used in cracking. High temperature oxidation/corrosion is a complex process and a mere change in the load bearing cross section is not the only result of these processes (Huff and Schreiber, 1972; Schmitt-Thomas, Meisel, and Dorn, 1978). Grain boundary attack, depletion of γ' precipitates, internal oxidation and sulphidation etc., reduce the strength of the alloy (Lobb and Nicholson, 1976; Le May, Truss and Sethi, 1969; Erdes and Denzier, 1979; Goebel and Pettit, 1970; Whittle, 1978). These corrosion induced mechanisms increase the cracking rate and reduce the time to rupture (Grunling, Illschner, Leistikow, Rahmel and Schmidt, 1978). Hence it is extremely important to evaluate the effects of hot corrosion and its interaction with enhanced stress concentration so that the mechanism can be well

understood for the proper selection of the alloy to a given application.

The aim of the present investigation is to assess the influence of vanadium in flue gases on the stress corrosion cracking and crack propagation in stainless steel under hot corrosive condition at 550°C.

EXPERIMENT

The chemical composition of the material 304 stainless steel and the base fuel kerosene used are given in Ref (Radhakrishnan, Iyer and Ramakrishna Iyer, 1982). The specimens were in the form of strips of 0.25 mm thick, 15 mm wide and 150 mm long. A sharp notch of depth 2.5 mm with a root radius of 0.1 mm was introduced on one edge of the specimen by electrospark machining.

A constant load lever type machine was used for the study. The details of the experimental set-up are schematically shown in Fig.1. The combustion conditions existing in gas turbines were simulated in a combustion chamber with the fuel injected under pressure. Vanadium at a pre-determined level was introduced into the kerosene base fuel in a soluble form. The specimen was loaded in tension and the high velocity flame was directed on the specimen. The temperature of the specimen was controlled at 550° ± 10 C by suitable adjustment of the burner and continuous monitoring of the specimen temperature by a chromel alumel thermocouple attached on the back side of the specimen.

Crack propagation was observed from the root of the machined notch and was measured by a travelling microscope with an accuracy of 0.01 mm. Crack initiation and propagation tests had been carried out at different stress levels and corrosive contents. The fractured surface of the specimen and the crack growth mode were analysed through optical and scanning electron microscopes.

RESULTS AND DISCUSSION

Variation of crack length with respect to time for 40 ppm of vanadium concentration and for different stress levels is shown in Fig. 2.

The results clearly demonstrate that with increasing stress levels cracking and crack propagation are more rapid. With increasing vanadium concentration upto around 20 ppm, crack growth increases. But beyond this level, there is slight decrease in the initiation time and also a decrease in the cracking rate. In general it has been observed that the entire cracking can be divided into a) nucleation, b) propagation and c) rapid fracture. A similar trend has been observed with sulphur as the corrosive (Radhakrishnan, Iyer and Ramakrishna Iyer, 1982).

Figure 3. shows the relation between the applied stress and the rupture time of the specimen at three vanadium levels. It can be observed that increasing vanadium content upto 20 ppm reduces the final rupture time of the material at any given stress level. But further increase in vanadium to 40 ppm does not seem to be as corrosive as is 20 ppm level. The rupture time shows a slight increase at 40 ppm level of vanadium. This clearly shows that there is a critical value of vanadium whose corrosive attack is the most aggressive one and this level appears to be around 20 ppm at 550°C. In general, the relation between stress and the rupture time t_r can be given by

$$\sigma = A (t_r/t_o)^\alpha \quad (1)$$

where the constants A and α depend on the vanadium concentration. The crack

growth data were fitted with a smooth curve which was differentiated to obtain the propagation rate da/dt at different crack lengths a . The load point deflection was measured; however, it was very small - of the order of 0.1 mm over the entire crack propagation range, thereby indicating that the crack propagation was not accompanied by gross deformation and the fracture mode appeared to be brittle. The crack propagation rate da/dt versus the stress intensity factor K is shown in Figure 4. Typical sigmoidal type of curves is obtained for different vanadium levels. At low stress intensity factors the curve becomes parallel to the Y-axis, which shows that there exists a threshold stress intensity factor K_{th} below which the crack may not propagate. The values of K_{th} for 10 ppm and 20 ppm vanadium are 2.8 MPa \sqrt{m} and 2.3 MPa \sqrt{m} . The value K_{th} corresponding to 40 ppm is 2.65 MPa \sqrt{m} , slightly higher than that of 20 ppm level, which again confirms that the critical vanadium content for most aggressive attack is around 20 ppm. The crack growth rate can be described best by an equation of the type (Radhakrishnan, Iyer and Ramakrishna Iyer, 1982).

$$da/dt = \frac{C}{E^2} (K^2 - K_{th}^2) \left(\frac{K_C}{K_C - K} \right) \quad (2)$$

The value of the constant C ranges from 50×10^4 to 80×10^4 h⁻¹ for the levels of vanadium used in the investigation.

The threshold stress intensity factor K_{th} can be looked upon as the limiting value below which the crack will not propagate under the particular conditions of loading. It is similar to K_{Isc} values evaluated under stress corrosion cracking. The K_{th} , however, may not be applicable for small sub-critical cracks, as has been noticed in the case of fatigue. To evaluate the sub-critical crack lengths below which the K_{th} has to be applied with great caution, the relation between the applied stress and the crack length has been computed and shown in Figure 5 on a log-log plot. As the crack length decreases, the stress level increases, but the increase cannot be beyond the creep strength of the material. In this particular case it is around 200 MPa. The intersection of the line corresponding to the creep strength with the line of stress versus crack length will give the limiting values of a_o below which application of K_{th} will not be valid. The relation between the limiting values of the sub-critical crack length a_o and vanadium level is shown in Figure 6. Here again we can notice that vanadium level of 20 ppm has the smallest sub-critical crack length a_o .

Extensive optical and scanning electron micrographic and fractographic studies have been carried out to understand the mechanism of corrosion attack. Figure 7 shows the optical micrograph of the sample attacked by combustion gases from kerosene. Except oxidation and isolated grain growth no special features are seen. Figures 8 and 9 are the SEM and optical micrographs of a failed specimen attacked by combustion gases containing 20 ppm vanadium. Isolated fusion along the lip could be seen (marked as A). Figure 10 is the optical micrograph of the same sample slightly away from the crack tip which shows isolated fusion with some grain growth. Far away from the crack lip the examination showed no fusion, but only isolated grain growth. Unetched micrograph of the same specimen is shown in Figure 11 which confirms the presence of fusion starting from crack lip.

Figures 12 and 13 show the micrographs of specimens for 10 ppm vanadium level, the former of the specimen that has withstood attack for more than 100 hrs at comparatively low loads and the latter of the specimen subjected to a higher load. In the first case practically no visible fusion has taken

place. The second case shows some fusion and grain growth. These indicate that a sufficiently large tensile stress is required to nucleate the local fusion. Similar effects can be seen in Figure 14 of specimen for 40 ppm vanadium level.

Phase diagram of $V_2O_5 - Cr_2O_3$ and Fe_2O_3 has shown to possess binary eutectics (Aurelio Burdese, 1964). V_2O_5 and Cr_2O_3 phase diagram shows a binary eutectic melting at $665^\circ C$ at a composition of 80% V_2O_5 and 20% Cr_2O_3 . V_2O_5 and Fe_2O_3 phase diagram shows an eutectic melting at $635^\circ C$ at a composition of 90% V_2O_5 and 10% Fe_2O_3 . Hence it is concluded that a ternary of V_2O_5 , Fe_2O_3 and Cr_2O_3 may occur whose melting point must be below $550^\circ C$. In order to investigate that possibility, compositions containing 90% V_2O_5 and differing percentages of Fe_2O_3 and Cr_2O_3 were mixed and melting point studies were carried out. These investigations have revealed that a composition containing 90% V_2O_5 , 6% Fe_2O_3 and 4% Cr_2O_3 melts between $480^\circ C$ and $485^\circ C$. Figure 15 shows the area of fusion (marked A) when a mixture of the above mentioned composition was placed on a stainless steel surface at $480^\circ C$.

From these tests it is concluded that localized fusion can take place at points where V_2O_5 comes in contact with Fe_2O_3 on the specimen. This is possible only in stressed areas where Cr_2O_3 protective films flake off giving rise to iron oxidation. A certain minimum stress is necessary for this flaking to take place. Also for compositions higher or lower than 90% V_2O_5 the temperatures of complete fusion are higher.

This can be a possible reason for the maximum attack when the vanadium level is around 20 ppm in the present investigation. Examination of failed samples revealed that fusion starts transgranularly and then becomes intergranular, indicating that the fusion zone is the point where Cr_2O_3 flakes off and it need not be at grain boundaries.

CONCLUSIONS

From the experimental investigations carried out to study the crack growth behaviour in 304 type stainless steel due to the presence of vanadium in combustion gases, the following conclusions have been made.

- Increase in vanadium content of the fuel upto 20 ppm reduces the crack initiation time and rupture life: thereafter the corrosive effect of vanadium decreases.
- The crack growth rate plotted against the LEFM parameter K yields a sigmoidal type of relation, thereby showing the presence of a threshold stress intensity factor K_{th} below which the crack may not propagate. The da/dt versus K relation can be described by an equation of the type

$$da/dt = C/E^2 (K^2 - K_{th}^2) \left(\frac{K_c}{K - K_c} \right)$$

The constant C varies from 50×10^4 to $80 \times 10^4 h^{-1}$ for the vanadium levels investigated.

- The threshold stress intensity factor K_{th} and the sub-critical crack length a_0 below which the threshold K_{th} may not be applicable, decrease with increasing vanadium concentration upto 20 ppm. At 40 ppm vanadium level a reverse trend is observed.
- Under the test condition of $550^\circ C$ there appears to be a critical vanadium

level for the worst possible attack. This level is around 20 ppm in the present investigation.

- The crack propagation is transgranular initially and then through grain boundaries due to the formation of low melting ternary eutectic of $V_2O_5 - Cr_2O_3 - Fe_2O_3$.

ACKNOWLEDGEMENT

Authors express their sincere thanks to Dr. V.S. Arunachalam, Scientific Adviser to Defence Minister and Director General, DRDO, New Delhi, for his constant encouragement. The work is part of the defence project No. DTT/70840/11/RD-82/4399/D(R&D). Thanks are due to Prof. P. Indiresan, Director IIT, Madras for his kind permission to present this paper.

REFERENCES

- Aurelio Burdese, (1964). 'System $Fe_2O_3 - V_2O_5$ ' and System $Cr_2O_3 - V_2O_5$ ' Phase diagram for ceramics, American Ceramic Society, 64.
- Erdes, E., and Denzier, E. (1979). Proc. Inter Conf on Behaviour of High Temp Alloys in aggressive Environments, Pattern, The Netherlands, 455.
- Goebel, J.A. and Pettit, F.S. (1970). Met Trans, 1, 3421.
- Grunling, H.W., Illschner, B., Leistikow, S., Rahmel, A. and Schmidt, M. (1978). Werkstoffe und Korrosion, 29, 601.
- Huff, H. and Schreiber, F. (1972). Werkstoffe und Korrosion, 23, 370.
- Le May, I., Truss, K.J., and Sethi, P.S. (1969). Trans ASME, J Basic Engg., 91, 575.
- Lobb, R.C., and Nicholson, R.D. (1976). Met Sci Engg., 22, 157.
- Radhakrishnan, V.M., K.J.L. Iyer, and Ramakrishna Iyer, S. (1982). Werkstoffe und Korrosion, 33, 461.
- Schmitt-Thomas, K.H., Meisel, H. and Dorn, H.J. (1978). Werkstoffe und Korrosion, 29, 1.
- Whittle, D.P. (1978). Proc Conf on High Temperature Alloys for Gas Turbines, COST, 50, 109.

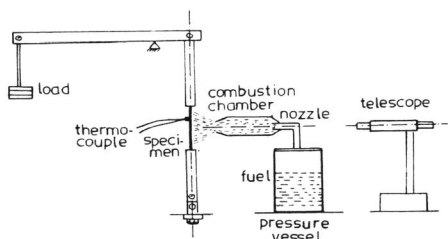


Fig. 1. Experimental set-up.

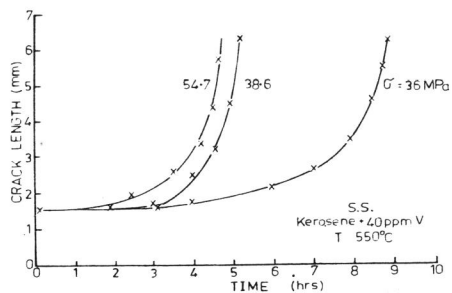


Fig. 2. Crack growth with time.

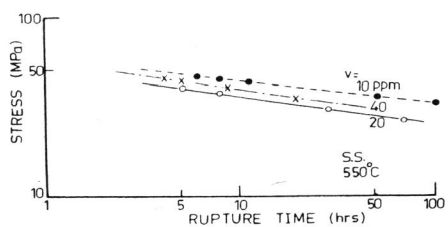


Fig. 3. Stress Vs rupture life.

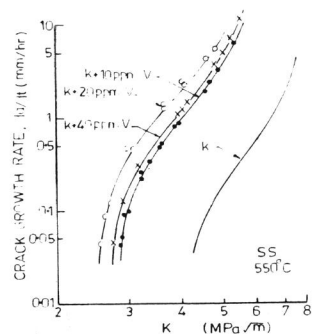


Fig. 4. da/dt Vs K .

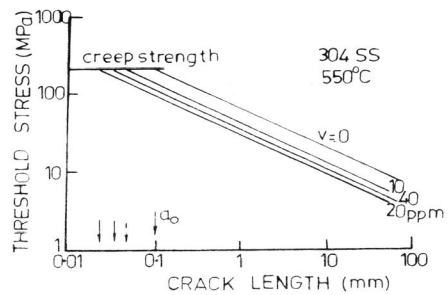


Fig. 5. Threshold stress Vs crack length.

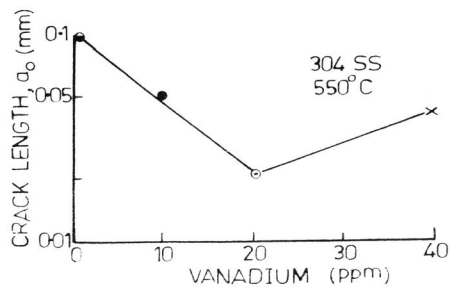


Fig. 6. Sub-critical crack length Vs vanadium level.

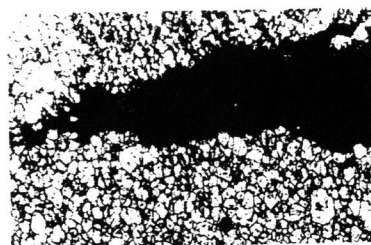
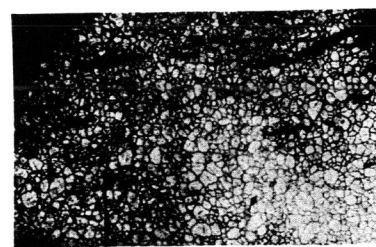


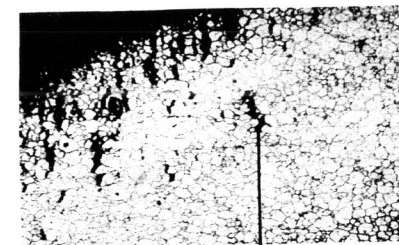
Fig. 7. Sample attacked by kerosene. X 200



Fig. 8. S E M of sample attacked by 20 ppm V. X 500



A



A

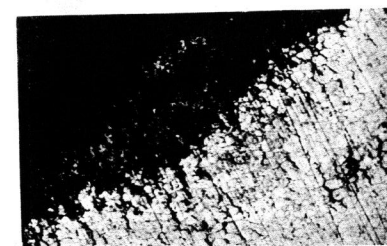


Fig. 9. Sample attacked by 20 ppm V showing isolated fusion. X 200.

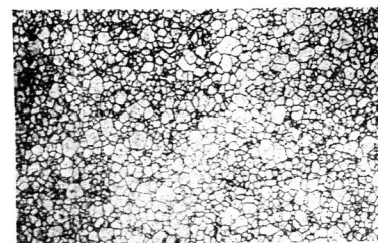


Fig. 10. Micrograph away from crack lip. X 200



Fig. 11. Unetched micrograph showing fusion. X 100.

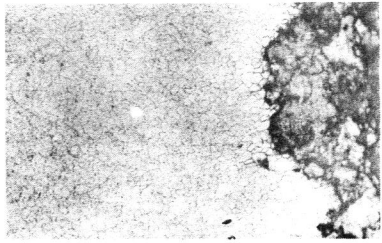


Fig. 12. Sample attacked by 10 ppm V. Low load. X 200.

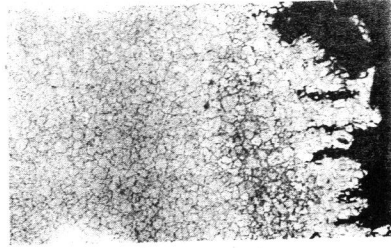


Fig. 13. Sample attacked by 10 ppm V. High load. X 200.

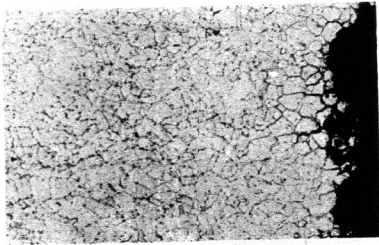


Fig. 14. Sample attacked by 40 ppm V. X 200.

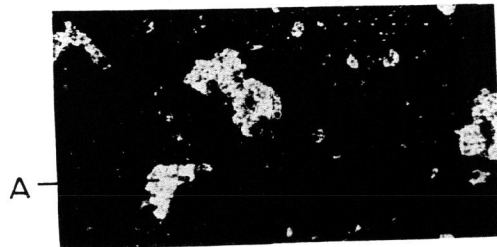


Fig. 15. Typical areas of fusion at 485°C. X 100